Quantum correlations through event horizons: Fermionic versus bosonic entanglement

Eduardo Martín-Martínez* and Juan León†
Instituto de Física Fundamental, CSIC Serrano 113-B, ES-28006 Madrid, Spain
(Received 25 January 2010; published 22 March 2010)

We disclose the behavior of quantum and classical correlations among all the different spatial-temporal regions of a space-time with an event horizon, comparing fermionic with bosonic fields. We show the emergence of conservation laws for entanglement and classical correlations, pointing out the crucial role that statistics plays in the information exchange (and more specifically, the entanglement tradeoff) across horizons. The results obtained here could shed new light on the problem of information behavior in noninertial frames and in the presence of horizons, giving better insight into the black-hole information paradox.

DOI: 10.1103/PhysRevA.81.032320 PACS number(s): 03.67.Mn, 03.65.Yz, 04.62.+v

I. INTRODUCTION

Relativistic quantum information, among other topics, analyzes entanglement behavior in noninertial settings. It combines tools from general relativity, quantum-field theory, and quantum-information theory. It is a new and fast-growing field [1–16]. Among its hot topics is the analysis of how the Unruh effect [17–20] affects the possible entanglement that an accelerated observer would share with an inertial observer.

For a bipartite entangled system, it is commonplace in relativistic quantum information to call the two observers Alice and Rob. We now consider that while the Alice proper frame is inertial, Rob undergoes a constant acceleration a.

It has been shown [4,5,15] that the Unruh effect degrades the entanglement between the two partners, thus affecting all the quantum-information tasks that they could perform. Specifically, it was demonstrated that as Rob accelerates, entanglement is completely degraded for a scalar field and, conversely, some degree of entanglement is preserved for fermionic fields. This behavior of fermionic fields has been proven to be universal [21], namely, it is independent of (i) the spin of the fermionic field, (ii) the kind of maximally entangled state from which we start, and (iii) the number of participating modes when going beyond the single-mode approximation (even an infinite number of them).

When Rob accelerates, the description of his partial state must be done by means of Rindler coordinates [19,22]. As shown below, when doing that, the description of the system splits into three different subsystems: Alice's Minkowskian system, a subsystem in region I of Rindler space-time (which we assign to Rob), and another subsystem, called AntiRob, constituted by the modes of the field in region IV of Rindler space-time.

It is important to note that Schwarzschild metrics in the neighborhood of the event horizon can be approximated by Rindler metrics. Therefore, an observer arbitrarily close to the Schwarzschild event horizon would correspond to an observer arbitrarily close to the Rindler horizon. Being arbitrarily close to the Rindler horizon is achieved when the acceleration parameter a goes to infinity. This would mean that the limit $a \to \infty$ of our analysis would correspond to a scenario in which Rob is resting arbitrarily close to the event horizon of a Schwarzschild black hole, while Alice is free-falling into it.

Any accelerated observer is constrained to either region I or IV of Rindler space-time. If we select region I coordinates to account for the accelerated observer Rob, he would remain causally disconnected from region IV, and therefore, Rob would be unable to communicate with the hypothetical observer AntiRob in region IV.

That means that to describe the point of view of Rob, we need to remove the part of the system on the other side of the event horizon. This is done by tracing over region IV of Rindler space-time, in other words, erasing the AntiRob information from the system. This partial tracing is the final step responsible for the entanglement degradation due to Unruh effect.

To gain a deeper understanding of those degradation mechanisms, it is useful to study how entanglement is lost as one traces over regions of the Rindler space-time. Although the system is obviously bipartite (Alice and Rob), in shifting to Rindler coordinates for Rob, the mathematical description of the system [4,5,15] admits a straightforward tripartition: Minkowskian modes (Alice), Rindler region I modes (Rob), and Rindler region IV modes (AntiRob).

In this paper, instead of considering only the Alice-Rob bipartition, we deal with all the different bipartitions of the system to study the correlation tradeoffs among them. These three bipartitions are

1. Alice-Rob (AR)
2. Alice-AntiRob ($A\bar{R}$)
3. Rob-AntiRob ($R\bar{R}$)

Bipartition 1 is the one most commonly considered in the literature. It represents the system formed by an inertial observer and the modes of the field which an accelerated observer is able to access.

The second bipartition represents the subsystem formed by the inertial observer Alice and the modes of the field which Rob is not able to access due to the presence of a horizon as he accelerates. The physical meaning of this bipartition can be more clearly understood in the limit $a \to \infty$, in which Rob is equivalent to an observer standing outside but arbitrarily close to a Schwarzschild black-hole event horizon. Then, the AntiRob subsystem represents the field modes inside the event horizon.

*martin@imaff.cfmac.csic.es
†leon@imaff.cfmac.csic.es; URL: http://www.imaff.csic.es/pcc/QUINFOG/

The third bipartition lacks physical meaning in terms of information theory, because communication between Rob and AntiRob is not allowed. Anyway, studying this bipartition is still useful to account for the correlations created between the spatial-temporal regions separated by an event horizon, and, therefore, its study is necessary and complementary to the previous ones in order to give a complete description of the information behavior across an event horizon.

In [5] the existence of these three possible bipartitions was considered only for spinless fermion fields. In this work, we will go far beyond the previous analysis and compare the correlation tradeoffs among different bipartitions for bosonic and fermionic fields, showing the leading role of statistics in the behavior of information on the proximity of event horizons.

The dimension of the Hilbert space for each mode has often been blamed as responsible for the difference between fermionic and bosonic entanglement behavior in the presence of horizons. Here we will disclose in which cases changing the dimension affects the correlation behavior, showing that, for the physical systems, it is largely irrelevant.

The work presented here will show that the role played by statistics in the comportment of information in the proximity of an event horizon is so important that it could even give a hint about the relationship between statistics and the black-hole information paradox.

This paper is organized as follows. In Sec. II we introduce some basic notions about an accelerated observer reference frame and present the Bogoliubov transformations which relate the Minkowskian modes of the fields with the analogous modes in Rindler coordinates. In Sec. III, we introduce some notation and present the vacuum and one-particle states for a scalar and a Dirac field as seen from an accelerated observer's point of view. We also write down the qubit states which we are going to analyze when one of the partners accelerates. In Sec. IV, we compute the quantum and classical correlations (in terms of mutual information and measures of quantum entanglement) for all the possible bipartitions of the system for a Dirac field, showing the emergence of an entanglement conservation law for the systems AR and $A\bar{R}$, as well as the conservation of classical correlations. In Sec. V, we repeat the same exercises for the case of scalar fields, finding striking differences which point out the enormous impact of statistics on correlation behavior. In both Secs. IV and V, we also analyze the correlations across the horizon, i.e., the $R\bar{R}$ system. Then we present our results and conclusions in Sec. VI.

II. SCALAR AND DIRAC FIELDS FROM CONSTANTLY ACCELERATED FRAMES

A uniformly accelerated observer viewpoint is described by means of the Rindler coordinates [22]. To cover the whole Minkowski space-time, two different sets of coordinates are necessary. These sets of coordinates define two causally disconnected regions in Rindler space-time. If we consider that the uniform acceleration a lies on the z axis, the new Rindler coordinates (t, x, y, z) as a function of Minkowski coordinates $(\tilde{t}, \tilde{x}, \tilde{y}, \tilde{z})$ are

$$a\tilde{t} = e^{az}\sinh(at), \quad a\tilde{z} = e^{az}\cosh(at), \quad \tilde{x} = x, \quad \tilde{y} = y, \tag{1}$$

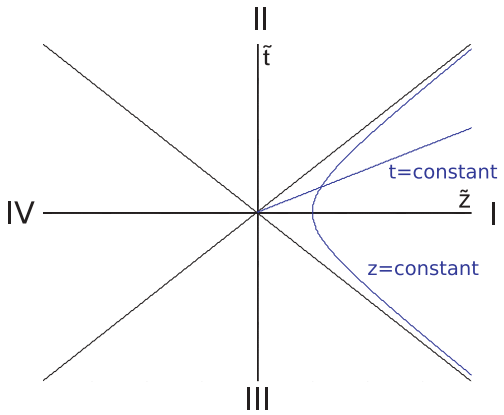

FIG. 1. (Color online) Rindler space-time diagram: lines of constant position $z = \text{const}$ are hyperbolas, and all the curves of constant proper time t for the accelerated observer are straight lines that come from the origin. A uniformly accelerated observer, Rob, travels along a hyperbola constrained to region I.

for region I, and

$$a\tilde{t} = -e^{az}\sinh(at), \quad a\tilde{z} = -e^{az}\cosh(at), \quad \tilde{x} = x, \quad \tilde{y} = y, \tag{2}$$

for region IV. As we can see from Fig. 1, although we have covered the whole Minkowski space-time with these sets of coordinates, there are two more regions labeled II and III. To map them, we would need to trade cosh by sinh in Eqs. (1) and (3). In these regions, t is a spacelike coordinate and z is a timelike coordinate. However, considering such regions is not required to describe fields from an accelerated observer's perspective [4,5,15,22,23].

The Rindler coordinates z, t go from $-\infty$ to ∞ independently in regions I and IV. It means that each region admits a separate quantization procedure with its corresponding positive and negative energy solutions of Klein-Gordon or Dirac equations[1] $\{\psi^{I+}_{k,s}, \psi^{I-}_{k,s}\}$ and $\{\psi^{IV+}_{k,s}, \psi^{IV-}_{k,s}\}$.

Particles and antiparticles will be classified with respect to the future-directed timelike Killing vector in each region. In region I, the future-directed Killing vector is

$$\partial^I_t = \frac{\partial\tilde{t}}{\partial t}\partial_{\tilde{t}} + \frac{\partial\tilde{z}}{\partial t}\partial_{\tilde{z}} = a(\tilde{z}\partial_{\tilde{t}} + \tilde{t}\partial_{\tilde{z}}), \tag{3}$$

whereas in region IV, the future-directed Killing vector is $\partial^{IV}_t = -\partial^I_t$.

This means that solutions in region I, having time dependence $\psi^{I+}_k \sim e^{-ik_0 t}$ with $k_0 > 0$, represent positive energy solutions; whereas solutions in region IV, having time dependence $\psi^{I+}_k \sim e^{-ik_0 t}$ with $k_0 > 0$, are actually negative energy solutions since ∂^{IV}_t points to the opposite direction of $\partial_{\tilde{t}}$. As I and IV are causally disconnected $\psi^{IV\pm}_{k,s}$ and $\psi^{I\pm}_{k,s}$ only have support in their own regions, vanishing outside them.

[1]Throughout this work we will consider that the spin of each mode lies in the acceleration direction and, hence, spin will not undergo Thomas precession due to instant Wigner rotations [5,24].

Let us denote $(a_{I,k}, a^\dagger_{I,k})$ for the scalar field and $(b_{I,k,s}, b^\dagger_{I,k,s})$ for the Dirac field as the particle annihilation and creation operators in region I, and $(c_{I,k,s}, c^\dagger_{I,k,s})$ the corresponding antiparticle Dirac field operators. Analogously we define $(a_{IV,k}, a^\dagger_{IV,k}, b_{IV,k,s}, b^\dagger_{IV,k,s}, c_{IV,k,s}, c^\dagger_{IV,k,s})$ as the particle and antiparticle operators in region IV.

The bosonic operators satisfy the commutation relations $[a_{\mathrm{R},k}, a^\dagger_{\mathrm{R}',k'}] = \delta_{\mathrm{R}\mathrm{R}'}\delta_{kk'}$ and the fermionic operators satisfy the anticommutation relations $\{c_{\mathrm{R},k,s}, c^\dagger_{\mathrm{R}',k',s'}\} = \delta_{\mathrm{R}\mathrm{R}'}\delta_{kk'}\delta_{ss'}$. The subscript R notates the Rindler region of the operator $\mathrm{R} = \{I, IV\}$. All other commutators and anticommutators are zero. This includes the anticommutators between operators in different regions of the Rindler space-time.

We can relate Minkowski and Rindler creation and annihilation operators by taking appropriate inner products and computing the so-called Bogoliubov coefficients [5,19,23,24]. For a scalar field, the Bogoliubov relationships for the annihilation operator of modes with positive frequency are

$$a_{M,k} = \cosh r_s a_{I,k} - \sinh r_s a^\dagger_{IV,-k}, \tag{4}$$

where

$$\tanh r_s = e^{-\pi \frac{k_0 c}{a}}. \tag{5}$$

For a Dirac field, the Bogoliubov relationships take the form

$$\begin{aligned} b_{M,k,s} &= \cos r_d b_{I,k,s} - \sin r_d c^\dagger_{IV,-k,-s}, \\ c^\dagger_{M,k,s} &= \cos r_d c^\dagger_{IV,k,s} + \sin r_d b_{I,-k,-s}, \end{aligned} \tag{6}$$

where

$$\tan r_s = e^{-\pi \frac{k_0 c}{a}}. \tag{7}$$

III. VACUUM AND ONE-PARTICLE STATES

The Minkowski vacuum state for the scalar field is defined by the tensor product of each frequency mode vacuum

$$|0\rangle = \bigotimes_k |0_k\rangle, \tag{8}$$

such that it is annihilated by a_k for all values of k. The Minkowski vacuum state for the Dirac field is defined by the tensor product of each frequency mode vacuum

$$|0\rangle = \bigotimes_{\substack{k,k' \\ s,s'}} |0_{k,s}\rangle^+ |0_{k',s'}\rangle^-, \tag{9}$$

such that it is annihilated by $b_{k,s}$ and $c_{k,s}$ for all values of k, s. The $\pm$ label indicates particle and antiparticle mode.

For the sake of this work, we are going to constrain ourselves to the single-mode approximation (SMA) [1,12]. In any case in [21] we showed, as a universality principle, that going beyond this approximation does not modify the way in which Unruh decoherence affects entanglement of spinless fermionic and Dirac fields. Specifically, it was shown that Unruh decoherence is independent of the number of modes of the field considered in the analysis, statistics being the ruler of this process. Hence, for our purposes, carrying out this approximation or not will not be relevant.

As shown in [4], the vacuum state for a k-momentum mode of a scalar field seen from the perspective of an accelerated observer is

$$|0_k\rangle_M = \frac{1}{\cosh r_s} \sum_{n=0}^{\infty} \tanh^n r_s |n_k\rangle_I |n_{-k}\rangle_{IV}, \tag{10}$$

and as shown in [15], the vacuum state for a Dirac field seen from the accelerated frame is

$$\begin{aligned} |0\rangle_M = \cos^2 r_d |0_k\rangle^+_I |0_k\rangle^-_{IV} + \sin r_d \cos r_d (|\uparrow_k\rangle^+_I |\downarrow_k\rangle^-_{IV} \\ + |\downarrow_k\rangle^+_I |\uparrow_k\rangle^-_{IV}) + \sin^2 r_d |p_k\rangle^+_I |p_k\rangle^-_{IV}, \end{aligned} \tag{11}$$

where $|p_k\rangle^\pm$ represents the pair of particles or antiparticles for frequency k as defined below. In these expressions, we use the same notation as in Refs. [4,15].

Notice that for fermions, there is a constraint due to the Pauli exclusion principle

$$b^\dagger_{k,s} b^\dagger_{k,s'} |0\rangle = |s s'_k\rangle \delta_{s,-s'}. \tag{12}$$

If $s = s'$ the two-particle state is not allowed. Therefore the allowed Minkowski states for each mode of particle or antiparticle are

$$\{|0_k\rangle^\pm, |\uparrow_k\rangle^\pm, |\downarrow_k\rangle^\pm, |p_k\rangle^\pm\}. \tag{13}$$

From now on, we will drop the sign $\pm$ because, in this work, a mode in region I will always be a particle mode and a mode in region IV will always represent an antiparticle mode. To simplify notation, we will also drop the k label, because we are working under the SMA.

We will use the following definitions for a pair of fermions:

$$\begin{aligned} |p\rangle_I &= b^\dagger_{I\uparrow} b^\dagger_{I\downarrow} |0\rangle_I = -b^\dagger_{I\downarrow} b^\dagger_{I\uparrow} |0\rangle_I, \\ |p\rangle_{IV} &= c^\dagger_{IV\uparrow} c^\dagger_{IV\downarrow} |0\rangle_{IV} = -c^\dagger_{IV\downarrow} c^\dagger_{IV\uparrow} |0\rangle_{IV}, \end{aligned} \tag{14}$$

and, being consistent with the different Rindler region operator anticommutation relations,

$$\begin{aligned} |s\rangle_I |s'\rangle_{IV} = b^\dagger_{Is} c^\dagger_{IVs'} |0\rangle_I |0\rangle_{IV} = -c^\dagger_{IVs'} b^\dagger_{Is} |0\rangle_I |0\rangle_{IV}, \\ c^\dagger_{IVs'} |s\rangle_I |0\rangle_{IV} = -|s\rangle_I |s'\rangle_{IV}. \end{aligned} \tag{15}$$

For this work, we will also need the Minkowskian one-particle state in Rindler coordinates. This state would be

$$|1\rangle_M = \frac{1}{\cosh^2 r_s} \sum_{n=0}^{\infty} \tanh^n r_s \sqrt{n+1} |n+1\rangle_I |n\rangle_{IV} \tag{16}$$

for the scalar field [4] and

$$\begin{aligned} |\uparrow\rangle_M &= \cos r_d |\uparrow\rangle_I |0\rangle_{IV} + \sin r_d |p\rangle_I |\uparrow\rangle_{IV}, \\ |\downarrow\rangle_M &= \cos r_d |\downarrow\rangle_I |0\rangle_{IV} - \sin r_d |p\rangle_I |\downarrow\rangle_{IV}, \end{aligned} \tag{17}$$

for the Dirac field [15].

Now we need to consider the following maximally entangled states in Minkowski coordinates:

$$|\Psi_s\rangle = \frac{1}{\sqrt{2}} (|0\rangle_M |0\rangle_M + |1\rangle_M |1\rangle_M), \tag{18}$$

$$|\Psi_d\rangle = \frac{1}{\sqrt{2}} (|0\rangle_M |0\rangle_M + |\uparrow\rangle_M |\downarrow\rangle_M). \tag{19}$$

These two maximally entangled states are analogous, both are qubit states and superpositions of the bipartite vacuum and

the bipartite one-particle state. The difference is that in (19) we have a Dirac field state, and hence, the one-particle states have spin.

For $|\Psi_d\rangle$, we have selected one among the possible values for the spin of the terms with one particle for Alice and Rob, but it can be shown that the election of a specific value for these spins is not relevant when considering the behavior of correlations. Then, the results presented here are independent of the particular choice of a spin state for the superposition (19).

IV. CORRELATIONS FOR THE DIRAC FIELD

The density matrix for whole tripartite state, which includes modes on both sides of the Rindler horizon along with Minkowskian modes, is built from (19)

$$\rho_d^{AR\bar{R}} = |\Psi_d\rangle\langle\Psi_d|. \tag{20}$$

The three different bipartitions for the Dirac field case are obtained by partial tracing over the part which we want to eliminate, that is,

$$\rho_d^{AR} = \mathrm{Tr}_{IV}\rho_d^{AR\bar{R}} = \sum_{s\in\{0,\uparrow,\downarrow,p\}} \langle s|_{IV}\rho_d^{AR\bar{R}}|s\rangle_{IV}, \tag{21}$$

$$\rho_d^{A\bar{R}} = \mathrm{Tr}_{I}\rho_d^{AR\bar{R}} = \sum_{s\in\{0,\uparrow,\downarrow,p\}} \langle s|_{I}\rho_d^{AR\bar{R}}|s\rangle_{I}, \tag{22}$$

$$\rho_d^{R\bar{R}} = \mathrm{Tr}_{M}\rho_d^{AR\bar{R}} = \sum_{s\in\{0,\uparrow,\downarrow,p\}} \langle s|_{M}\rho_d^{AR\bar{R}}|s\rangle_{M}. \tag{23}$$

And the density matrix for each individual subsystem is obtained by tracing over the other subsystems:

$$\rho_d^{A} = \mathrm{Tr}_{I}\rho_d^{AR} = \mathrm{Tr}_{IV}\rho_d^{A\bar{R}}, \tag{24}$$

$$\rho_d^{R} = \mathrm{Tr}_{IV}\rho_d^{R\bar{R}} = \mathrm{Tr}_{M}\rho_d^{AR}, \tag{25}$$

$$\rho_d^{\bar{R}} = \mathrm{Tr}_{I}\rho_d^{R\bar{R}} = \mathrm{Tr}_{M}\rho_d^{A\bar{R}}. \tag{26}$$

The different bipartitions are characterized by the following density matrices:

$$\begin{aligned}\rho_d^{AR} = {} & \tfrac{1}{2}[\cos^4 r_d|00\rangle\langle 00| + \sin^2 r_d\cos^2 r_d(|0\uparrow\rangle\langle 0\uparrow| \\ & + |0\downarrow\rangle\langle 0\downarrow|) + \sin^4 r_d|0p\rangle\langle 0p| + \cos^3 r_d(|00\rangle \\ & \times\langle\uparrow\downarrow| + |\uparrow\downarrow\rangle\langle 00|) - \sin^2 r_d\cos r_d(|0\uparrow\rangle\langle\uparrow p| \\ & + |\uparrow p\rangle\langle 0\uparrow|) + \cos^2 r_d|\uparrow\downarrow\rangle\langle\uparrow\downarrow| + \sin^2 r_d \\ & \times|\uparrow p\rangle\langle\uparrow p|],\end{aligned} \tag{27}$$

$$\begin{aligned}\rho_d^{A\bar{R}} = {} & \tfrac{1}{2}[\cos^4 r_d|00\rangle\langle 00| + \sin^2 r_d\cos^2 r_d(|0\downarrow\rangle\langle 0\downarrow| \\ & + |0\uparrow\rangle\langle 0\uparrow|) + \sin^4 r_d|0p\rangle\langle 0p| - \sin^3 r_d \\ & \times(|0p\rangle\langle\uparrow\downarrow| + |\uparrow\downarrow\rangle\langle 0p|) + \sin r_d\cos^2 r_d(|0\uparrow\rangle \\ & \times\langle\uparrow,0| + |\uparrow 0\rangle\langle 0\uparrow|) + \cos^2 r_d|\uparrow 0\rangle\langle\uparrow 0| \\ & + \sin^2 r_d|\uparrow\downarrow\rangle\langle\uparrow\downarrow|],\end{aligned} \tag{28}$$

$$\begin{aligned}\rho_d^{R\bar{R}} = {} & \tfrac{1}{2}[\cos^4 r_d|00\rangle\langle 00| + \sin r_d\cos^3 r_d \\ & \times(|00\rangle\langle\uparrow\downarrow| + |00\rangle\langle\downarrow\uparrow| + |\uparrow\downarrow\rangle\langle 00| + |\downarrow\uparrow\rangle\langle 00|) \\ & + \sin^2 r_d\cos^2 r_d(|00\rangle\langle p,p| + |\uparrow\downarrow\rangle\langle\uparrow\downarrow| \\ & + |\uparrow\downarrow\rangle\langle\downarrow\uparrow| + |\downarrow\uparrow\rangle\langle\uparrow\downarrow| + |\downarrow\uparrow\rangle\langle\downarrow\uparrow| \\ & + |p,p\rangle\langle 00|) + \sin^3 r_d\cos r_d(|\uparrow\downarrow\rangle\langle p,p| \\ & + |p,p\rangle\langle\uparrow\downarrow| + |\downarrow\uparrow\rangle\langle p,p| + |p,p\rangle\langle\downarrow\uparrow|) \\ & + \cos^2 r_d|\downarrow 0\rangle\langle\downarrow 0| + \sin^2 r_d|p\downarrow\rangle\langle p\downarrow| \\ & - \cos r_d\sin r_d(|\downarrow 0\rangle\langle p\downarrow| + |p\downarrow\rangle\langle\downarrow 0|) \\ & + \sin^4 r_d|pp\rangle\langle pp|],\end{aligned} \tag{29}$$

where the bases are

$$|nm\rangle = |n^A\rangle_M|m^R\rangle_I, \tag{30}$$

$$|nm\rangle = |n^A\rangle_M|m^{\bar{R}}\rangle_{IV}, \tag{31}$$

$$|nm\rangle = |n^R\rangle_I|m^{\bar{R}}\rangle_{IV}, \tag{32}$$

respectively, for (27)–(29).

On the other hand, the density matrices for the individual subsystems (24)–(26) are

$$\begin{aligned}\rho_d^{R} = {} & \tfrac{1}{2}[\sin^2 r_d(1+\sin^2 r_d)|p\rangle\langle p| + \sin^2 r_d\cos^2 r_d|\uparrow\rangle\langle\uparrow| \\ & + \cos^2 r_d(1+\sin^2 r_d)|\downarrow\rangle\langle\downarrow| + \cos^4 r_d|0\rangle\langle 0|],\end{aligned} \tag{33}$$

$$\begin{aligned}\rho_d^{\bar{R}} = {} & \tfrac{1}{2}[\cos^2 r_d(1+\cos^2 r_d)|0\rangle\langle 0| + \sin^2 r_d\cos^2 r_d|\uparrow\rangle\langle\uparrow| \\ & + \sin^2 r_d(1+\cos^2 r_d)|\downarrow\rangle\langle\downarrow| + \sin^4 r_d|p\rangle\langle p|],\end{aligned} \tag{34}$$

$$\rho_d^{A} = \tfrac{1}{2}(|0\rangle\langle 0| + |\uparrow\rangle\langle\uparrow|). \tag{35}$$

A. Mutual information: Creation, exchange, and conservation

Mutual information accounts for the correlations (both quantum and classical) between two different parts of a system. It is defined as

$$I_{AB} = S_A + S_B - S_{AB}, \tag{36}$$

where S_A, S_B, and S_{AB} are, respectively, the von Neumann entropies for the individual subsystems A and B and for the joint system AB. To compute the mutual information for each bipartition we will need the eigenvalues of the corresponding density matrices. We will go through the entire process step by step in the lines below.

1. Bipartition Alice-Rob

The eigenvalues of the matrix for the Alice-Rob system (27) are

$$\begin{aligned}\lambda_1 &= \lambda_2 = 0,\\ \lambda_3 &= \tfrac{1}{2}\sin^2 r_d\cos^2 r_d,\\ \lambda_4 &= \tfrac{1}{2}\sin^4 r_d,\\ \lambda_5 &= \tfrac{1}{2}\cos^2 r_d(1+\cos^2 r_d),\\ \lambda_6 &= \tfrac{1}{2}\sin^2 r_d(1+\cos^2 r_d).\end{aligned} \tag{37}$$

2. Bipartition Alice-AntiRob

The eigenvalues of the matrix for the Alice-AntiRob system (28) are

$$\begin{aligned}\lambda_1 &= \lambda_2 = 0,\\ \lambda_3 &= \tfrac{1}{2}\sin^2 r_d\cos^2 r_d,\\ \lambda_4 &= \tfrac{1}{2}\cos^4 r_d,\\ \lambda_5 &= \tfrac{1}{2}\sin^2 r_d(1+\sin^2 r_d),\\ \lambda_6 &= \tfrac{1}{2}\cos^2 r_d(1+\sin^2 r_d).\end{aligned} \tag{38}$$

3. Bipartition Rob-AntiRob

All the eigenvalues of the matrix for the Rob-AntiRob system (29) are zero, except two of them:

$$\lambda_1 = \lambda_2 = \tfrac{1}{2}, \quad \lambda_{i>2} = 0. \tag{39}$$

4. Von Neumann entropies for each subsystem and mutual information

To compute the von Neumann entropies, we need the eigenvalues of every bipartition and the individual density matrices. The eigenvalues of ρ_d^{AR}, $\rho_d^{A\bar{R}}$, and $\rho_d^{R\bar{R}}$ are, respectively (37), (38), and (39). The eigenvalues of the individual system density matrices can be directly read from (33), (34), and (35), since ρ_s^R, $\rho_s^{\bar{R}}$, and ρ_s^A have diagonal forms in the given basis. The von Neumann entropy for partition B of the system is

$$S_B = -\mathrm{Tr}(\rho \log_2 \rho) = -\sum \lambda_i \log_2 \lambda_i. \tag{40}$$

At this point, computing the entropies is quite straightforward. The von Neumann entropies for all the partial systems are

$$\begin{aligned} S_R &= 1 - \sin^2 r_d \log_2(\sin^2 r_d) - \frac{3}{2}\cos^2 r_d \log_2(\cos^2 r_d) \\ &\quad - \frac{1+\sin^2 r_d}{2}\log_2(1+\sin^2 r_d), \\ S_{\bar{R}} &= 1 - \cos^2 r_d \log_2(\cos^2 r_d) - \frac{3}{2}\sin^2 r_d \log_2(\sin^2 r_d) \\ &\quad - \frac{1+\cos^2 r_d}{2}\log_2(1+\cos^2 r_d), \\ S_{AR} &= S_{\bar{R}}, \quad S_{A\bar{R}} = S_R, \quad S_{R\bar{R}} = S_A = 1. \end{aligned} \tag{41}$$

And then, the mutual information for all possible bipartitions of the system will be

$$\begin{aligned} I_{AR} &= S_A + S_R - S_{AR} = 1 + S_R - S_{\bar{R}}, \\ I_{A\bar{R}} &= S_A + S_{\bar{R}} - S_{A\bar{R}} = 1 + S_{\bar{R}} - S_R, \\ I_{R\bar{R}} &= S_R + S_{\bar{R}} - S_{R\bar{R}} = S_R + S_{\bar{R}} - 1. \end{aligned}$$

At first glance, we can see a conservation law of the mutual information for the Alice-Rob and Alice-AntiRob systems:

$$I_{AR} + I_{A\bar{R}} = 2, \tag{42}$$

which suggests a correlations transfer from the Alice-Rob to the Alice-AntiRob system as the acceleration increases.

Figure 2 shows the behavior of the mutual information for the three bipartitions. It also shows how the correlations across the horizon (Rob and AntiRob) increase, up to a certain finite limit, as Rob accelerates.

If we recall the results on spinless fermion fields [5], we see that the results for Alice-Rob and Alice-AntiRob are exactly the same as those obtained in [5], being that the conservation law obtained here is also valid for that spinless fermion case. This result was expected according to the universality argument adduced in [21] as the explanation for the Unruh decoherence for fermion fields of arbitrary spin.

However, something different occurs with the Rob-AntiRob system. The creation of correlations between modes on both sides of the horizon is greater in the Dirac field case. This is related to the dimension of the Hilbert space. As we will see in more detail later, the dimension of the Hilbert space plays a determinant role only in the comportment of the Rob-AntiRob correlations.

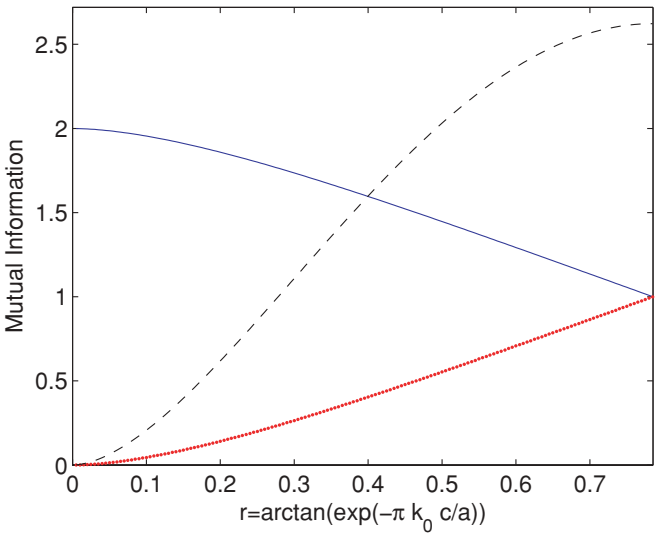

FIG. 2. (Color online) Dirac field: Mutual information tradeoff and conservation law between the Alice-Rob (AR, blue solid line) and Alice-AntiRob ($A\bar{R}$, red dotted line) systems as acceleration varies. It also shows the behavior of mutual information for the Rob-AntiRob system ($R\bar{R}$, black dashed line).

B. Entanglement conservation and behavior across the horizon

We will use the negativity to account for the distillable entanglement of the different bipartitions of the system. Negativity is an entangle monotone which is only sensitive to distillable entanglement and is defined as the sum of the negative eigenvalues of the partially transposed density matrix for the system, which is defined as the transpose of only one of the subsystem qudits in the bipartite density matrix. If σ_i are the eigenvalues of ρ_{AB}^{pT}, then

$$\mathcal{N}_{AB} = \frac{1}{2}\sum_i (|\sigma_i| - \sigma_i) = -\sum_{\sigma_i<0} \sigma_i. \tag{43}$$

Therefore, to compute it, we will need the partial transposition of the bipartite density matrices (27), (28), and (29), which we will notate as η_d^{AR}, $\eta_d^{A\bar{R}}$, and $\eta_d^{R\bar{R}}$, respectively.

$$\begin{aligned} \eta_d^{AR} &= \tfrac{1}{2}[\cos^4 r_d |00\rangle\langle 00| + \sin^2 r_d \cos^2 r_d (|0\uparrow\rangle\langle 0\uparrow| \\ &\quad + |0\downarrow\rangle\langle 0,\downarrow|) + \sin^4 r_d |0p\rangle\langle 0p| + \cos^3 r_d \\ &\quad \times (|0\downarrow\rangle\langle\uparrow,0| + |\uparrow 0\rangle\langle 0,\downarrow|) - \sin^2 r_d \cos r_d \\ &\quad \times (|0p\rangle\langle\uparrow\uparrow| + |\uparrow\uparrow\rangle\langle 0p|) + \cos^2 r_d |\uparrow\downarrow\rangle\langle\uparrow\downarrow| \\ &\quad + \sin^2 r_d |\uparrow p\rangle\langle\uparrow p|], \end{aligned} \tag{44}$$

$$\begin{aligned} \eta_d^{A\bar{R}} &= \tfrac{1}{2}[\cos^4 r_d |00\rangle\langle 00| + \sin^2 r_d \cos^2 r_d (|0\downarrow\rangle\langle 0\downarrow| \\ &\quad + |0\uparrow\rangle\langle 0\uparrow|) + \sin^4 r_d |0p\rangle\langle 0p| - \sin^3 r_d \\ &\quad \times (|0\downarrow\rangle\langle\uparrow p| + |\uparrow p\rangle\langle 0\downarrow|) + \sin r_d \cos^2 r_d \\ &\quad \times (|00\rangle\langle\uparrow\uparrow| + |\uparrow\uparrow\rangle\langle 00|) + \cos^2 r_d |\uparrow 0\rangle\langle\uparrow 0| \\ &\quad + \sin^2 r_d |\uparrow\downarrow\rangle\langle\uparrow\downarrow|], \end{aligned} \tag{45}$$

$$\begin{aligned}\eta_d^{R\bar{R}} = {} & \tfrac{1}{2}[\cos^4 r_d|00\rangle\langle 00| + \sin r_d \cos^3 r_d(|0\downarrow\rangle\langle\uparrow 0| \\ & + |0\uparrow\rangle\langle\downarrow 0| + |\uparrow 0\rangle\langle 0\downarrow| + |\downarrow 0\rangle\langle 0\uparrow|) + \sin^2 r_d \\ & \times \cos^2 r_d(|0p\rangle\langle p0| + |\uparrow\downarrow\rangle\langle\uparrow\downarrow| + |\uparrow\uparrow\rangle\langle\downarrow\downarrow| \\ & + |\downarrow\downarrow\rangle\langle\uparrow\uparrow| + |\downarrow\uparrow\rangle\langle\downarrow\uparrow| + |p0\rangle\langle 0p|) + \sin^3 r_d \\ & \times \cos r_d(|\uparrow p\rangle\langle p\downarrow| + |p\downarrow\rangle\langle\uparrow p| + |\downarrow p\rangle\langle p\uparrow| \\ & + |p\uparrow\rangle\langle\downarrow p|) + \cos^2 r_d|\downarrow 0\rangle\langle\downarrow 0| + \sin^2 r_d|p\downarrow\rangle \\ & \times \langle p\downarrow| - \cos r_d \sin r_d(|\downarrow\downarrow\rangle\langle p0| + |p0\rangle\langle\downarrow\downarrow|) \\ & + \sin^4 r_d|pp\rangle\langle pp|]. \end{aligned} \tag{46}$$

In the following subsections we will compute the negativity for each bipartition of the system.

1. Bipartition Alice-Rob

The eigenvalues of the partially transposed density matrix for the bipartition Alice-Rob (44) turn out to be

$$\begin{aligned} \lambda_1 &= \frac{1}{2}\cos^4 r_d, \quad \lambda_2 = \frac{1}{2}\cos^2 r \sin^2 r_d, \\ \lambda_3 &= \frac{1}{2}\sin^2 r_d, \quad \lambda_4 = \frac{1}{2}\cos^2 r_d, \\ \lambda_{5,6} &= \frac{1}{4}\sin^2 r_d \cos^2 r_d \left(1 \pm \sqrt{1 + \frac{4\cos^2 r_d}{\sin^4 r}}\right), \\ \lambda_{7,8} &= \frac{1}{4}\sin^4 r_d \left(1 \pm \sqrt{1 + \frac{4\cos^2 r_d}{\sin^4 r_d}}\right). \end{aligned} \tag{47}$$

As we can see, λ_8 is nonpositive and λ_6 is negative for all values of a; therefore, the state will always preserve some degree of distillable entanglement. The negativity is, after some basic algebra,

$$\mathcal{N}_d^{AR} = \tfrac{1}{2}\cos^2 r_d. \tag{48}$$

2. Bipartition Alice-AntiRob

The eigenvalues of the partially transposed density matrix for the bipartition Alice-AntiRob (45) turn out to be

$$\begin{aligned} \lambda_1 &= \frac{1}{2}\sin^4 r_d, \quad \lambda_2 = \frac{1}{2}\sin^2 r_d \cos^2 r_d, \\ \lambda_3 &= \frac{1}{2}\cos^2 r_d, \quad \lambda_4 = \frac{1}{2}\sin^2 r_d, \\ \lambda_{5,6} &= \frac{1}{4}\sin^2 r_d \cos^2 r_d \left(1 \pm \sqrt{1 + \frac{4\tan^2 r_d}{\cos^2 r_d}}\right), \\ \lambda_{7,8} &= \frac{1}{4}\cos^4 r_d \left(1 \pm \sqrt{1 + \frac{4\tan^2 r_d}{\cos^2 r_d}}\right). \end{aligned} \tag{49}$$

The negativity, after some basic algebra, turns out to be

$$\mathcal{N}_d^{A\bar{R}} = \tfrac{1}{2}\sin^2 r_d. \tag{50}$$

It is remarkable—and constitutes one of the most suggestive results of this article—that we have obtained here a conservation law for the Alice-Rob and Alice-AntiRob entanglements, since the sum of both negativities is independent of the accelerations, i.e.,

$$\mathcal{N}_d^{A\bar{R}} + \mathcal{N}_d^{AR} = \tfrac{1}{2}. \tag{51}$$

This is similar to the result (42) for mutual information. Again, one could check that for spinless fermion fields, the same conservation law (51) obtained here applies. This was again expected due to the universality principle demonstrated in [21].

As we will see below, this conservation of quantum correlations is exclusive of fermionic fields. Statistics can be blamed for this neat result. This is in line with what was suggested in [21], since nothing of the sort will be found for bosonic fields.

3. Bipartition Rob-AntiRob

The eigenvalues of the partially transposed density matrix for the bipartition Rob-AntiRob (46) turn out to be

$$\begin{aligned} \lambda_1 &= \frac{\cos^4 r_d}{2}, \quad \lambda_2 = \frac{\sin^4 r_d}{2}, \\ \lambda_3 &= \lambda_4 = \frac{\sin^2 r_d \cos^2 r_d}{2}, \\ \lambda_{5,6} &= \pm\frac{\sin r_d \cos^3 r_d}{2}, \\ \lambda_{7,8} &= \pm\frac{\cos r_d \sin^3 r_d}{2}, \\ \lambda_{9,10} &= \frac{\cos^2 r_d}{4}(1 \pm \sqrt{1 + \sin^2(2r_d)}), \\ \lambda_{11,12} &= \frac{\sin^2 r_d}{4}(1 \pm \sqrt{1 + \sin^2(2r_d)}), \\ \lambda_{13,14,15,16} &= \pm\frac{\sin(2r_d)}{8}(1 \pm \sqrt{1 + \sin^2(2r_d)}), \end{aligned} \tag{52}$$

and, therefore, the sum of the negative eigenvalues gives a negativity

$$\mathcal{N}_d^{R\bar{R}} = \frac{1}{4}\left[\frac{\sin(2r_d)}{2} - 1 + [1 + \sin(2r_d)]\sqrt{1 + \sin^2(2r_d)}\right]. \tag{53}$$

As can be seen from (53) and graphically in Fig. 3, the entanglement between Rob and AntiRob, created as Rob accelerates, grows up to a finite value. Although this entanglement is useless for quantum-information tasks because of the impossibility of classical communication between both sides of an event horizon, the result obtained here is a useful hint in understanding how information behaves in the proximity of horizons.

Comparing again this result with spinless fermions [5], we see that for Dirac fields, the maximum value of the negativity is greater. Again this is strongly related to the dimension of the Hilbert space, as we will comment on more deeply below, when we deal with scalar fields.

V. CORRELATIONS FOR THE SCALAR FIELD

The density matrix for the whole tripartite state, which includes modes in both sides of the horizon along with Minkowskian modes, is built from (18):

$$\rho_s^{AR\bar{R}} = |\Psi_s\rangle\langle\Psi_s| \tag{54}$$

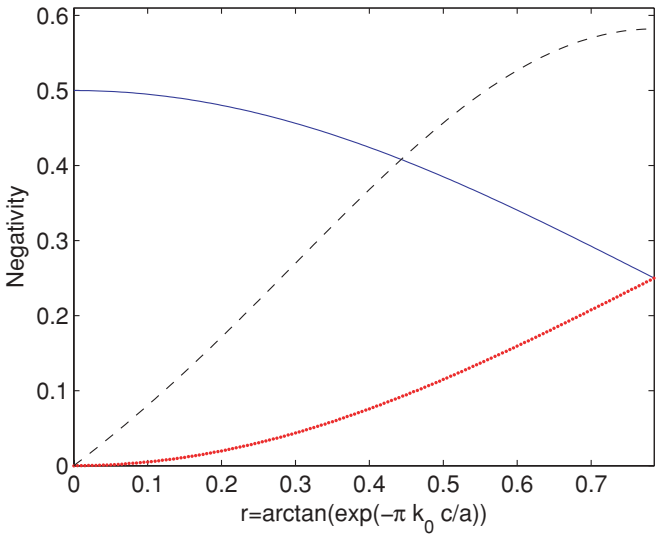

FIG. 3. (Color online) Same as Fig. 2, but showing negativity tradeoff and conservation law between the AR and $A\bar{R}$ systems as acceleration varies, and the behavior of the quantum correlations for the $R\bar{R}$ system.

As in the fermion case, the three different bipartitions for the scalar field case are obtained as follows:

$$\rho_s^{AR} = \mathrm{Tr}_{IV}\rho_s^{AR\bar{R}}, \tag{55}$$

$$\rho_s^{A\bar{R}} = \mathrm{Tr}_{I}\rho_s^{AR\bar{R}}, \tag{56}$$

$$\rho_s^{R\bar{R}} = \mathrm{Tr}_{M}\rho_s^{AR\bar{R}}, \tag{57}$$

and the density matrix for each individual subsystem is

$$\rho_s^{A} = \mathrm{Tr}_{I}\rho_s^{AR} = \mathrm{Tr}_{IV}\rho_s^{A\bar{R}}, \tag{58}$$

$$\rho_s^{R} = \mathrm{Tr}_{IV}\rho_s^{R\bar{R}} = \mathrm{Tr}_{M}\rho_s^{AR}, \tag{59}$$

$$\rho_s^{\bar{R}} = \mathrm{Tr}_{I}\rho_s^{R\bar{R}} = \mathrm{Tr}_{M}\rho_s^{A\bar{R}}. \tag{60}$$

The bipartite systems are characterized by the following density matrices:

$$\rho_s^{AR} = \sum_{n=0}^{\infty}\frac{\tanh^{2n} r_s}{2\cosh^2 r_s}\left[|0n\rangle\langle 0n| + \frac{\sqrt{n+1}}{\cosh r_s}(|0n\rangle\langle 1n+1| + |1n+1\rangle\langle 0n|) + \frac{n+1}{\cosh^2 r_s}|1n+1\rangle\langle 1n+1|\right], \tag{61}$$

$$\rho_s^{A\bar{R}} = \sum_{n=0}^{\infty}\frac{\tanh^{2n} r_s}{2\cosh^2 r_s}\left[|0n\rangle\langle 0n| + \frac{\sqrt{n+1}}{\cosh r_s}\tanh r_s(|0n+1\rangle\times\langle 1n| + |1n\rangle\langle 0n+1|) + \frac{n+1}{\cosh^2 r_s}|1n\rangle\langle 1n|\right], \tag{62}$$

$$\rho_s^{R\bar{R}} = \sum_{\substack{n=0\\m=0}}^{\infty}\frac{\tanh^{n+m} r_s}{2\cosh^2 r_s}\left(|nn\rangle\langle mm| + \frac{\sqrt{n+1}\sqrt{m+1}}{\cosh^2 r_s}\times|n+1n\rangle\langle m+1m|\right), \tag{63}$$

where the bases are, respectively,

$$|nm\rangle = |n^A\rangle_M|m^R\rangle_I, \tag{64}$$

$$|nm\rangle = |n^A\rangle_M|m^{\bar{R}}\rangle_{IV}, \tag{65}$$

$$|nm\rangle = |n^R\rangle_I|m^{\bar{R}}\rangle_{IV}, \tag{66}$$

for (61), (62), and (63).

On the other hand, the density matrices for the individual subsystems (58), (59), and (60) are

$$\rho_s^R = \sum_{n=0}^{\infty}\frac{\tanh^{2(n-1)} r_s}{2\cosh^2 r_s}\left(\tanh^2 r_s + \frac{n}{\cosh^2 r_s}\right)|n\rangle\langle n|, \tag{67}$$

$$\rho_s^{\bar{R}} = \sum_{n=0}^{\infty}\frac{\tanh^{2n} r_s}{2\cosh^2 r_s}\left(1 + \frac{n+1}{\cosh^2 r_s}\right)|n\rangle\langle n|, \tag{68}$$

$$\rho_s^{A} = \frac{1}{2}(|0\rangle\langle 0| + |1\rangle\langle 1|). \tag{69}$$

A. Mutual information: Creation, exchange, and conservation

Mutual information accounts for the correlations (both quantum and classical) between two different parts of the system. Its definition is (36).

To compute the mutual information for each bipartition, we will need the eigenvalues of the corresponding density matrices. We will go through the entire process in detail in the lines below.

1. Bipartition Alice-Rob

The density matrix for the Alice-Rob system (61) consists of an infinite number of 2×2 blocks in the basis $\{|0n\rangle, |1n+1\rangle\}_{n=0}^{\infty}$ which have the form

$$\frac{\tanh^{2n} r_s}{2\cosh^2 r_s}\begin{pmatrix} 1 & \frac{\sqrt{n+1}}{\cosh r_s} \\ \frac{\sqrt{n+1}}{\cosh r_s} & \frac{n+1}{\cosh^2 r_s}\end{pmatrix}, \tag{70}$$

and whose eigenvalues are

$$\lambda_n^1 = 0, \qquad \lambda_n^2 = \frac{\tanh^{2n} r_s}{2\cosh^2 r_s}\left(1 + \frac{n+1}{\cosh^2 r_s}\right). \tag{71}$$

2. Bipartition Alice-AntiRob

Except for the diagonal element corresponding to $|00\rangle\langle 00|$ (which forms a 1×1 block itself), the density matrix for the Alice-AntiRob system (62) consists of an infinite number of 2×2 blocks in the basis $\{|0n\rangle, |1n-1\rangle\}_{n=1}^{\infty}$ which have the form

$$\frac{\tanh^{2n} r_s}{2\cosh^2 r_s}\begin{pmatrix} 1 & \frac{\sqrt{n}}{\sinh r_s} \\ \frac{\sqrt{n}}{\sinh r_s} & \frac{n}{\sinh^2 r_s}\end{pmatrix}. \tag{72}$$

We can gather all the eigenvalues in the following expression:

$$\lambda_n^1 = \frac{\tanh^{2n} r_s}{2\cosh^2 r_s}\left(1 + \frac{n}{\sinh^2 r_s}\right), \qquad \lambda_n^2 = 0. \tag{73}$$

3. Bipartition Rob-AntiRob

It is easy to see that the density matrix for Rob-AntiRob (63), which basically consists of the direct sum of two blocks of infinite dimension, only has rank $\mathrm{rank}(\rho_s^{R\bar{R}}) = 2$. Therefore its eigenvalues are zero except for two of them, which are

$$\lambda_1^{R\bar{R}} = \sum_{n=0}^{\infty} \frac{\tanh^{2n} r_s}{2\cosh^2 r_s} = \frac{1}{2},$$
$$\lambda_2^{R\bar{R}} = \sum_{n=0}^{\infty} \frac{(n+1)\tanh^{2n} r_s}{2\cosh^4 r_s} = \frac{1}{2}. \tag{74}$$

So, the von Neumann entropy for $\rho^{R\bar{R}}$ is

$$S^{R\bar{R}} = 1. \tag{75}$$

4. Von Neumann entropies for each subsystem and mutual information

To compute the von Neumann entropies, we need the eigenvalues of every bipartition and the individual density matrices. The eigenvalues of ρ_s^{AR}, $\rho_s^{A\bar{R}}$, and $\rho_s^{R\bar{R}}$ are, respectively, (71), (73), and (74).

The eigevalues of the individual systems density matrices can be directly read from (67), (68), and (69), since ρ_s^R, $\rho_s^{\bar{R}}$, and ρ_s^A have diagonal forms in the Fock basis. The von Neumann entropy for a partition B of the system is (40).

At this point, computing the entropies is quite straightforward. Von Neumann entropy for the Rob partial system is

$$S_R = -\sum_{n=0}^{\infty} \frac{\tanh^{2(n-1)} r_s}{2\cosh^2 r_s}\left(\tanh^2 r_s + \frac{n}{\cosh^2 r_s}\right) \times \log_2\left[\frac{\tanh^{2(n-1)} r_s}{2\cosh^2 r_s}\left(\tanh^2 r_s + \frac{n}{\cosh^2 r_s}\right)\right]. \tag{76}$$

The partial matrices have a similar mathematical structure. Therefore, we can express the nontrivial entropies for all the possible partitions as a function of the entropy (76) for Rob's partial system

$$S_{\bar{R}} = \frac{S_R}{\tanh^2 r_s} - \frac{1}{2\sinh^2 r_s}\log_2\left(\frac{1}{2\cosh^2 r_s}\right) + \log_2(\tanh^2 r_s),$$
$$S_{AR} = S_{\bar{R}}, \quad S_{A\bar{R}} = S_R, \quad S_{R\bar{R}} = S_A = 1. \tag{77}$$

Notice that the expression for $S_{\bar{R}}$ may appear to blow up as $r_s \to 0$; however, this is not the case, and it can be checked analytically using (76) that $\lim_{r\to 0} S_{\bar{R}} = 0$.

The mutual information for all possible bipartitions of the system will be

$$I_{AR} = S_A + S_R - S_{AR} = 1 + S_R - S_{\bar{R}},$$
$$I_{A\bar{R}} = S_A + S_R - S_{A\bar{R}} = 1 + S_{\bar{R}} - S_R,$$
$$I_{R\bar{R}} = S_R + S_{\bar{R}} - S_{R\bar{R}} = S_R + S_{\bar{R}} - 1.$$

Again we obtain a conservation law of the mutual information for the Alice-Rob and Alice-AntiRob system

$$I_{AR} + I_{A\bar{R}} = 2, \tag{78}$$

which again suggests a correlations transfer from the Alice-Rob to the Alice-AntiRob system as the acceleration increases.

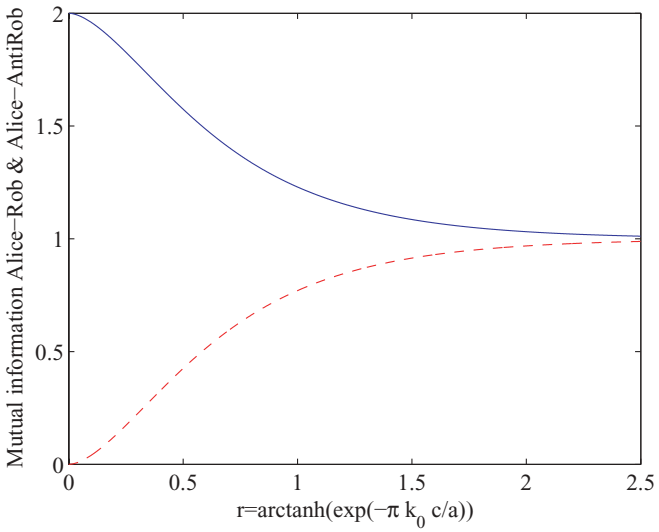

FIG. 4. (Color online) Scalar field: Mutual information tradeoff and conservation law between the AR (blue solid line) and $A\bar{R}$ (red dashed line) systems.

Although the conservation law is the same as for fermion fields (42), the specific dependance of the mutual information with the acceleration is different, as can be seen in Fig. 4. Later, when we analyze the negativity for all the bipartitions, we will see that even though mutual information fulfills this conservation law, we must wait for the analysis of quantum correlations to appreciate the striking differences between fermions and bosons.

Figure 5 shows how the correlations across the horizon (Rob and AntiRob) increase with no bound as Rob accelerates. This unbounded growth is not only strongly related with the infinite dimension of the Hilbert space, but also very much influenced by statistics. As we will see later, we require the infinite dimension of the bosons' Hilbert space in order to have correlations $R\bar{R}$ which survive the limit $a \to \infty$. That

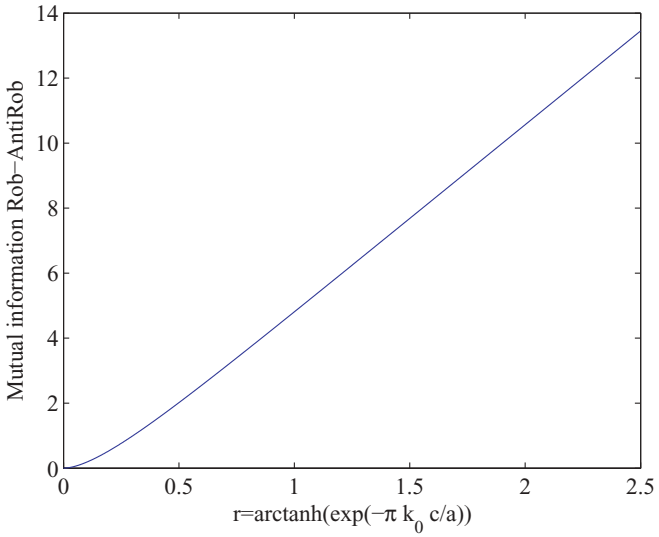

FIG. 5. (Color online) Scalar field: Behavior of the mutual information for the $R\bar{R}$ system as acceleration varies.

is not the case for fermions, where those correlations survive the limit even though the Hilbert space has finite dimension. We will discuss how the infinite dimension is responsible for the unbounded growth of correlations across the horizon after studying the negativity in Sec. V B.

B. Entanglement behavior across the horizon

As we did above, we will compute the negativity (43) for the scalar case. To compute it, we need the partial transposition of the bipartite density matrices (61), (62) and (63), which we will notate as η_s^{AR}, $\eta_s^{A\bar{R}}$, and $\eta_s^{R\bar{R}}$, respectively.

$$\eta_s^{AR} = \sum_{n=0}^{\infty} \frac{\tanh^{2n} r_s}{2\cosh^2 r_s} \left[|0n\rangle\langle 0n| + \frac{\sqrt{n+1}}{\cosh r_s}(|0n+1\rangle\langle 1n| + |1n\rangle\langle 0n+1|) + \frac{n+1}{\cosh^2 r_s}|1n+1\rangle\langle 1n+1| \right], \tag{79}$$

$$\eta_s^{A\bar{R}} = \sum_{n=0}^{\infty} \frac{\tanh^{2n} r_s}{2\cosh^2 r_s} \left[|0n\rangle\langle 0n| + \frac{\sqrt{n+1}}{\cosh r_s}\tanh r_s(|0n\rangle \times \langle 1n+1| + |1n+1\rangle\langle 0n|) + \frac{n+1}{\cosh^2 r_s}|1n\rangle\langle 1n| \right], \tag{80}$$

$$\eta_s^{R\bar{R}} = \sum_{\substack{n=0\\m=0}}^{\infty} \frac{\tanh^{n+m} r_s}{2\cosh^2 r_s} \left(|nm\rangle\langle mn| + \frac{\sqrt{n+1}\sqrt{m+1}}{\cosh^2 r_s} \times |n+1m\rangle\langle m+1n| \right). \tag{81}$$

In the following subsections we will compute the negativity of each bipartition of the system.

1. Bipartition Alice-Rob

Except for the diagonal element corresponding to $|00\rangle\langle 00|$ (which forms a 1×1 block itself), the partial transposition of the density matrix ρ_s^{AR} (79) has a 2×2 block structure in the basis $\{|0n+1\rangle, |1n\rangle\}$, that is,

$$\frac{\tanh^{2n} r_s}{2\cosh^2 r_s} \begin{pmatrix} \tanh^2 r_s & \frac{\sqrt{n+1}}{\cosh r_s} \\ \frac{\sqrt{n+1}}{\cosh r_s} & \frac{n}{\sinh^2 r_s} \end{pmatrix}. \tag{82}$$

Hence, the eigenvalues of (79) are

$$\lambda^1 = \frac{1}{2\cosh^2 r_s},$$
$$\lambda_n^2 = \frac{\tanh^{2n} r_s}{4\cosh^2 r_s} \left[\left(\frac{n}{\sinh^2 r_s} + \tanh^2 r_s \right) \pm \sqrt{\left(\frac{n}{\sinh^2 r_s} + \tanh^2 r_s \right)^2 + \frac{4}{\cosh^2 r_s}} \right]. \tag{83}$$

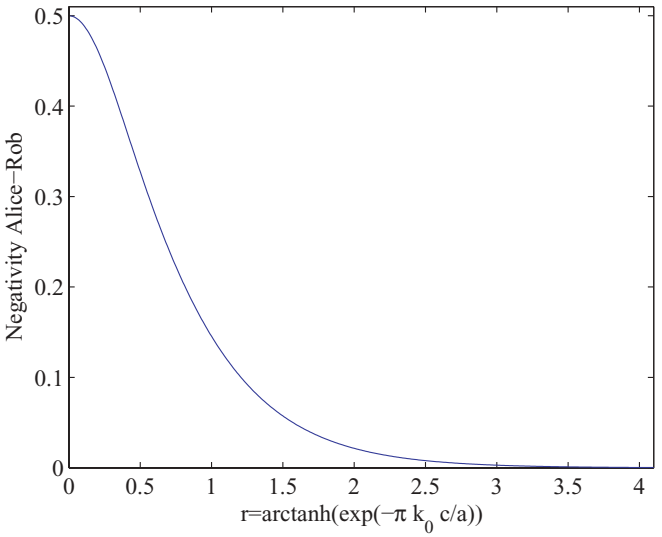

FIG. 6. (Color online) Scalar field: Behavior of the negativity for the AR bipartition as Rob accelerates.

And then the negativity for this bipartition is

$$\mathcal{N}_s^{AR} = \sum_{n=0}^{\infty} \frac{\tanh^{2n} r_s}{4\cosh^2 r_s} \left| \left(\frac{n}{\sinh^2 r_s} + \tanh^2 r_s \right) - \sqrt{\left(\frac{n}{\sinh^2 r_s} + \tanh^2 r_s \right)^2 + \frac{4}{\cosh^2 r_s}} \right|. \tag{84}$$

Figure 6 shows $\mathcal{N}_s^{AR}$ as a function of r_s.

2. Bipartition Alice-AntiRob

Except for the diagonal element corresponding to $|10\rangle\langle 10|$ (which forms a 1×1 block itself), the partial transposition of the density matrix $\rho_s^{A\bar{R}}$ (80) has a 2×2 block structure in the basis $\{|0n\rangle, |1n+1\rangle\}$:

$$\frac{\tanh^{2n} r_s}{2\cosh^2 r_s} \begin{pmatrix} 1 & \frac{\tanh r_s}{\cosh r_s}\sqrt{n+1} \\ \frac{\tanh r_s}{\cosh r_s}\sqrt{n+1} & \frac{\tanh^2 r_s}{\cosh^2 r_s}(n+2) \end{pmatrix}. \tag{85}$$

Hence, the eigenvalues of (80) are

$$\lambda^1 = \frac{1}{2\cosh^4 r_s},$$
$$\lambda_n^2 = \frac{\tanh^{2n} r_s}{4\cosh^2 r_s} \left[\left(1 + (n+2)\frac{\tanh^2 r_s}{\cosh^2 r_s} \right) \pm \sqrt{\left(1 + (n+2)\frac{\tanh^2 r_s}{\cosh^2 r_s} \right)^2 - \frac{4\tanh^2 r_s}{\cosh^2 r_s}} \right]. \tag{86}$$

Therefore, the negativity for this bipartition is always 0, independently of the value of Rob's acceleration. The important implications of this striking result are discussed below.

3. Bipartition Rob-AntiRob

The partial transposition of the density matrix $\rho_s^{R\bar{R}}$ (81) has a block structure, but the blocks themselves are of

different dimensions which grow up to infinity. Because of this, negativity is not as easily computed as for the other cases, since it is not possible to write it in a closed form.

However, it is still possible to numerically compute the eigenvalues of (81) taking into account that the blocks forming the matrix are endomorphisms that act in the subspace expanded by the basis $B_D = \{|mn\rangle\}$ in which $m+n = D-1 =$ constant; that is, the first block acts within the subspace expanded by the basis $B_1 = \{|00\rangle\}$, the second $B_2 = \{|01\rangle, |10\rangle\}$, the third $B_3 = \{|02\rangle, |20\rangle, |11\rangle\}$, the fourth $B_4 = \{|03\rangle, |30\rangle, |12\rangle, |21\rangle\}$, and so forth. In this fashion, the whole matrix is an endomorphism within the subspace $\bigoplus_{i=1}^{\infty} S_i$, with S_i the subspace (of dimension $D = i$) expanded by the basis B_i.

Let us denote as M_D the blocks that form the matrix (81), with D the dimension of each block. Then its structure is

$$M_D = \begin{pmatrix} 0 & a_1 & 0 & 0 & \cdots & \cdots & \cdots & 0 \\ a_1 & 0 & a_2 & 0 & \cdots & \cdots & \cdots & 0 \\ 0 & a_2 & 0 & a_3 & \cdots & \cdots & \cdots & 0 \\ 0 & 0 & a_3 & 0 & a_4 & \cdots & \cdots & 0 \\ 0 & 0 & 0 & \ddots & \ddots & \ddots & \cdots & 0 \\ \vdots & \vdots & \vdots & \vdots & \ddots & \ddots & \ddots & \vdots \\ 0 & 0 & 0 & 0 & \cdots & \ddots & 0 & a_{D-1} \\ 0 & 0 & 0 & 0 & 0 & \ldots & a_{D-1} & a_D \end{pmatrix}, \tag{87}$$

which is to say, the diagonal terms are zero except for the last one, and the rest of the matrix elements are zero except for the two diagonals on top and underneath the principal diagonal. The elements a_n are defined as follows:

$$a_{2l+1} = \frac{(\tanh r_s)^{D-1}}{2\cosh^2 r_s}, \tag{88}$$

$$a_{2l} = \sqrt{D-l}\sqrt{l}\frac{(\tanh r_s)^{D-2}}{2\cosh^4 r_s}. \tag{89}$$

Notice that the elements are completely different when the value of the label n is odd or even.

As the whole matrix is the direct sum of the blocks

$$\eta_s^{R\bar{R}} = \bigoplus_{D=1}^{\infty} M_D, \tag{90}$$

the eigenvalues and, specifically, the negative eigenvalues of $\eta_s^{R\bar{R}}$ would be the negative eigenvalues of all the blocks M_D gathered together. It can be shown that the absolute value of the negative eigenvalues of the blocks decreases quickly as the dimension increases. Thus, the negativity $\mathcal{N}_s^{R\bar{R}}$ converges promptly to a finite value for a given value of r_s. Figure 7 shows the behavior of $\mathcal{N}_s^{R\bar{R}}$ with r_s, showing that the entanglement increases unboundedly between Rob and AntiRob.

Let us compare these results with the fermion case. First, as shown in [5], the negativity of the Alice-Rob system decreases as Rob accelerates, vanishing in the limit $a \to \infty$, instead of remaining finite as in the fermionic cases [5,15].

What may be more surprising is the behavior of the quantum correlations of the Alice-AntiRob system. In the fermion case, negativity grows monotonically from zero (for $a = 0$) to a finite value (for $a = \infty$). Nevertheless, for scalars, Alice-AntiRob negativity is identically zero for all acceleration. Hence, there is no transfer of entanglement from Alice-Rob to Alice-AntiRob as was the case for fermions. Still, correlations (classical) are not lost, as can be concluded from (78).

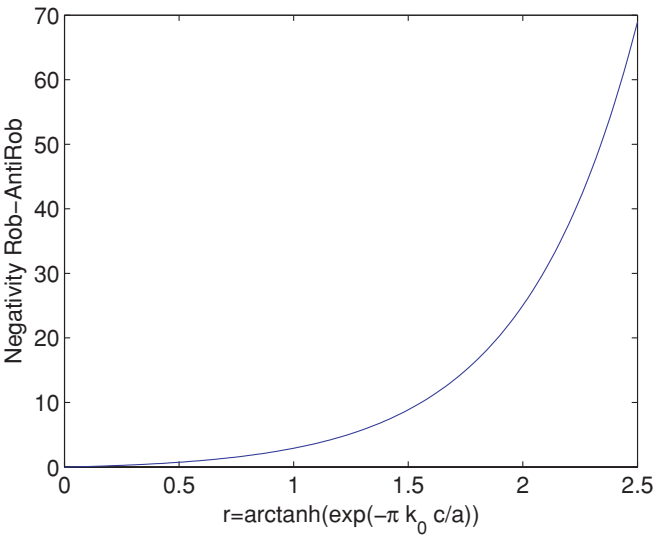

FIG. 7. (Color online) Scalar field: Behavior of negativity for the bipartition Rob-AntiRob as Rob accelerates.

Why do we obtain such loss of entanglement for the bosonic case and, conversely, it does not happen in the fermionic case? The answer is, once again, statistics.

One could think of the infinite dimensionality of the Hilbert space for scalars (compared to the finite dimension for fermions) as the cause of this different behavior. However, we will prove that it has to do with the bosonic nature of the field rather than with the infinite dimensionality of the Hilbert space. We can see this considering hardcore bosons instead of scalars, which is to say, we can limit the occupation number for the bosonic modes to a certain finite limit N instead of taking $N \to \infty$. By doing so, we transform the infinite dimension Hilbert space for bosons into a finite dimension one. As we will see below, in any case, the negativity would continue being zero for all a.

To illustrate this argument, we could compare the fermionic case with the hardcore bosonic case with $N = 2$ which would be its analog, namely, a bosonic field whose occupation number is limited to 2. Looking at the partially transposed density matrix for the fermionic case, we can seek for the negative eigenvalues origin and then compare the analogous structure that would appear for the hardcore bosonic case. We will see that in the latter case, no negative eigenvalues are obtained.

Recalling the form of matrix (45), we can see that it has a structure of four 1×1 blocks, which give positive eigenvalues, and two 2×2 blocks, which are the ones whose eigenvalues contribute to the negativity. These two blocks are

$$\frac{1}{2}\begin{pmatrix} \cos^4 r_d & \sin r_d \cos^2 r_d \\ \sin r_d \cos^2 r_d & 0 \end{pmatrix} \tag{91}$$

in the basis $\{|00\rangle, |\uparrow\uparrow\rangle\}$ and

$$\frac{1}{2}\begin{pmatrix} \sin^2 r_d \cos^2 r_d & -\sin^3 r_d \\ -\sin^3 r_d & 0 \end{pmatrix} \tag{92}$$

in the basis $\{|0\downarrow\rangle, |\uparrow p\rangle\}$.

For hardcore bosons with occupation number limited to $n = N$, the structure would be quite similar to (80), but this time we would have two 1×1 blocks instead of one (the elements $|00\rangle\langle 00|$ and $|NN\rangle\langle NN|$) and $N2 \times 2$ blocks with the structure (85) but with $n = 0, \ldots, N-1$. Specifically, for $N = 2$, the two blocks are

$$\frac{1}{2\cosh^2 r_s}\begin{pmatrix} 1 & \frac{\tanh r_s}{\cosh r_s} \\ \frac{\tanh r_s}{\cosh r_s} & \frac{2\tanh^2 r_s}{\cosh^2 r_s} \end{pmatrix} \tag{93}$$

in the basis $\{|00\rangle, |11\rangle\}$ and

$$\frac{\tanh^2 r_s}{2\cosh^2 r_s}\begin{pmatrix} 1 & \frac{\sqrt{2}\tanh r_s}{\cosh r_s} \\ \frac{\sqrt{2}\tanh r_s}{\cosh r_s} & \frac{3\tanh^2 r_s}{\cosh^2 r_s} \end{pmatrix} \tag{94}$$

in the basis $\{|01\rangle, |12\rangle\}$.

The key difference comes from the second diagonal term of the blocks, which in the fermionic case, it is impossible to obtain due to the peculiar structure that fermionic statistics imposes on (18). On the other hand, for bosons this term is nonzero, and furthermore it has a value large enough to prevent the partially transposed density matrix from having negative eigenvalues.

As mentioned in Sec. III, this result is independent of the election of the particular value for the spin components for Alice and Rob in (19). It also does not depend on N (the limit for occupation number we impose on hardcore boson modes), and this phenomenon is exclusively ruled by statistics. Besides, this is evidence of the difference between hardcore bosons and fermions, which sometimes in the literature are considered the same. This is not the case in terms of quantum correlations, for which we have observed that statistics is a key feature.

This is additional confirmation of the important role that statistics plays in the behavior of correlations in noninertial frames, and specifically in the proximity of black holes. In fact, getting closer and closer to the Rindler horizon (i.e., $a \to \infty$), the situation resembles more and more the scenario in which Rob is arbitrarily close to the event horizon of a Schwarzschild black hole, while Alice is free-falling into it.

About the bipartition Rob-AntiRob, at first glance at Figs. 5 and 7 one would think that there might be some inconsistency between the behavior of entanglement and mutual information, as the latter grows linearly while negativity seems to grow exponentially. Since mutual information accounts for all the correlations (quantum and classical) between Rob and AntiRob, the result may appear paradoxical. However, these apparently inconsistent results are due to the fact that negativity cannot be identified as the entanglement itself, but rather as a monotone that grows along with the degree of entanglement. The specific functional form chosen for the monotone is not imposed by physical motivations. Actually, we could have chosen logarithmic negativity, instead of negativity, as our entanglement monotone since it is in fact better for comparing with mutual information because of its additive properties [25].

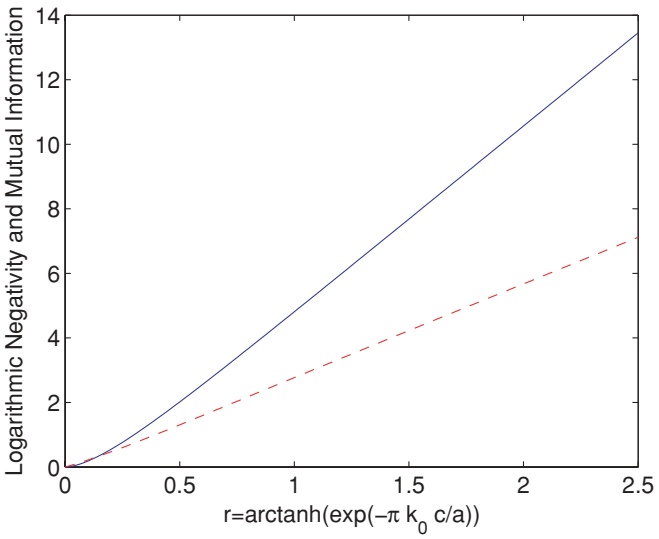

FIG. 8. (Color online) Scalar field: Comparison of growth of quantum and all (quantum+classical) correlations for the Rob-AntiRob system as acceleration increases. Quantum correlations are accounted for by logarithmic negativity (red dashed line). This figure compares this entanglement measurement with mutual information (blue solid line).

The result obtained in this case, shown in Fig. 8, is that when acceleration grows both growths become linear.

Coming back to the basic argument of this paper, we observe that entanglement grows unboundedly for this bipartition, converse to the fermion case in which negativity increases up to a certain finite limit as Rob accelerates. This different behavior is not only related to the dimension of the Hilbert space but also strongly influenced by statistics.

Actually, if we consider again hardcore bosons, we can see from (87) that limiting the dimension would give a finite number of blocks which contribute to the negativity, being the last one truncated and having dimension $N-1$ instead of $N+1$. In any case, taking the limit $a \to \infty$, we can see that negative eigenvalues of the partially transposed density matrix tend to zero as a grows. Therefore negativity vanishes in that limit.

Naturally, the same happened in the standard bosonic case, but then negativity was the sum of an infinite number of terms, each vanishing when $a \to \infty$. The negativity resulted in being divergent, though. Now we are adding only a finite number of vanishing terms so that negativity, which was divergent when $a \to \infty$ for standard bosons, now vanishes in such limit. This behavior contrasts with the fermionic case and the standard scalar field case.

This and other points related to the impact of dimension and statistics on these correlations across the horizon will be discussed elsewhere.

VI. CONCLUSIONS

This work focused on the bipartite correlations between different spatial-temporal domains in the presence of an event horizon. Specifically, we analyzed all the possible bipartitions of an entangled system composed of an inertial observer and an accelerated one, which inhabits a universe with an event horizon.

As pointed out in the Introduction, Rindler space-time is the simplest case which, presenting a horizon, also reproduces two interesting physical scenarios. Namely, it describes the point of view of an uniformly accelerated observer and, in the limit $a \to \infty$, it reproduces an observer resting arbitrarily close to a Schwarzschild black-hole event horizon.

First of all, we studied the relation between the behavior of entanglement of the Alice-Rob and Alice-AntiRob system, which are the two bipartitions to which one could assign physical meaning. We have shown that the dimension of the Hilbert space has little to do with the entanglement behavior.

We recall two results to support this statement: on one hand, in [21] we studied the case of a Dirac and a spinless fermion field beyond the single-mode approximation in which fermionic Hilbert space turned out to have infinite dimension. On the other hand, here we have analyzed bosons in a Hilbert space of infinite and finite dimensions (scalar field and hardcore scalar, respectively). The results are that the characteristic differences between fermion fields and bosonic fields for the bipartitions AR and $A\bar{R}$ manifest independently of the dimension of the Hilbert space.

Here we have disclosed a great difference in the behavior of quantum correlations for fermions and bosons. In the fermionic case, we showed that at the same time as Unruh decoherence destroys the entanglement of the Alice-Rob system, entanglement is created between Alice and AntiRob. This means that the quantum entanglement lost between Alice and the field modes outside the event horizon is gained between Alice and the modes inside. This is expressed through the entanglement conservation law (51), which we deduced for fermions.

Nevertheless, for bosonic states, it was shown that as acceleration increases, entanglement is quickly and completely lost between Alice and Rob, while no quantum correlations are created between Alice and AntiRob. Moreover, no entanglement of any kind survives among any physical bipartition of the system in the limit $a \to \infty$ for the bosonic case. This contrasts with the fermionic case, where the amount of entanglement among all the physical bipartitions of the system remains always constant.

These observations are in accord with previous work [21], in which we suggested that all entanglement which survives a black-hole event horizon is purely statistical and gives no further information than the statistical correlations which inescapably appear due to the fermionic nature of the field.

These powerful and suggestive results may well be related to what was obtained in such previous works as [26,27]. In those works it was demonstrated, for pure states in first quantization, that the fact of considering indistinguishable fermions implies that there are quantum correlations of which we cannot get rid due to the antisymmetrization of the fermionic wave functions. Of course, the scenario here is not the same, but analyzing together the results obtained here and those in [26,27] reveals the somewhat special feature of fermionic fields regarding entanglement comportment: statistics information, or in this case, information of the fermionic nature of the field, cannot be erased from our system, and still, that information is expressed by means of quantum correlations.

Another remarkable result is the conservation law for mutual information for fermions (42) and bosons (78) shown in in Figs. 2 and 4. The detailed behavior is different for both cases, but the same conservation law is obtained for the mutual information of the bipartitions Alice-Rob and Alice-AntiRob. Mutual information accounts for both classical and quantum correlations (despite the fact that in general there is no trivial relation between negativity and mutual information). However, for the bosonic case, the mutual information distributes between the Alice-Rob and Alice-AntiRob systems more rapidly than for the fermion case.

This result for mutual information means that correlations are always conserved for the Alice-Rob and Alice-AntiRob systems, despite the fact that quantum correlations vanish for the bosonic case and are preserved (and this is the effect of statistics) in the fermionic case. The fact that classical correlations behave in a similar way for fermions and bosons while quantum correlations comport so differently suggests again that the quantum entanglement which survives the black-hole limit is merely statistical.

Another difference between fermions and bosons appears in analyzing the correlations between modes inside and outside the horizon. It is interesting to notice that as the noninertial partner accelerates, correlations across the horizon are created. Both the dimension of the Hilbert space and statistics play a fundamental role in the behavior of these correlations. We have obtained that for Dirac fields, these correlations, quantum and classical, grow as Rob accelerates up to a finite value at the limit $a \to \infty$. This limit is greater than the analogous limit obtained for spinless fermions in [5] whose Hilbert space for each mode is smaller. For the bosonic case, on the contrary, those correlations grow unboundedly, being infinite when $a \to \infty$. Surprisingly, for the hardcore bosonic field, in which Hilbert space has an arbitrarily large but finite dimension, the behavior of this correlations is not even monotonical, being zero for the inertial limit as well as for the infinite acceleration regime, but nonzero in between. Therefore, statistics and dimensionality must be taken into account in order to find the origin of this comportment.

We have dealt with this bipartition separately since it cannot be given a physical interpretation in terms of information theory. However, it is worthwhile to analyze its comportment, since it could reveal the relative roles of dimensionality and statistics when accounting for the behavior of correlations in the presence of an event horizon. This topic, which deserves further study, is expected to appear elsewhere.

It is important to recall that the limit $a \to \infty$ can be understood as considering an observer moving in a trajectory arbitrarily close to the event horizon of a Schwarzschild black hole [4]. So, along with the interest of describing the correlations between accelerated observers, this study gives further insight into the fate of correlations in the presence of a black hole. Together with the results of [21], our results could be of use in tackling the problem of the information paradox in black holes, for which they indicate that statistics plays a very important role.

ACKNOWLEDGMENTS

This work was partially supported by the Spanish MICINN Project FIS2008-05705/FIS and by the CAM research consortium QUITEMAD S2009/ESP-1594. E. M.-M. was partially supported by a CSIC JAE-PREDOC2007 Grant.

[1] P. M. Alsing and G. J. Milburn, Phys. Rev. Lett. **91**, 180404 (2003).
[2] H. Terashima and M. Ueda, Phys. Rev. A **69**, 032113 (2004).
[3] Y. Shi, Phys. Rev. D **70**, 105001 (2004).
[4] I. Fuentes-Schuller and R. B. Mann, Phys. Rev. Lett. **95**, 120404 (2005).
[5] P. M. Alsing, I. Fuentes-Schuller, R. B. Mann, and T. E. Tessier, Phys. Rev. A **74**, 032326 (2006).
[6] J. L. Ball, I. Fuentes-Schuller, and F. P. Schuller, Phys. Lett. A **359**, 550 (2006).
[7] G. Adesso, I. Fuentes-Schuller, and M. Ericsson, Phys. Rev. A **76**, 062112 (2007).
[8] K. Brádler, Phys. Rev. A **75**, 022311 (2007).
[9] Y. Ling, S. He, W. Qiu, and H. Zhang, J. Phys. A **40**, 9025 (2007).
[10] D. Ahn, Y. Moon, R. Mann, and I. Fuentes-Schuller, J. High Energy Phys. 06 (2008) 062.
[11] Q. Pan and J. Jing, Phys. Rev. D **78**, 065015 (2008).
[12] P. M. Alsing, D. McMahon, and G. J. Milburn, J. Opt. B **6**, S834 (2004).
[13] J. Doukas and L. C. L. Hollenberg, Phys. Rev. A **79**, 052109 (2009).
[14] G. Ver Steeg and N. C. Menicucci, Phys. Rev. D **79**, 044027 (2009).
[15] J. León and E. Martín-Martínez, Phys. Rev. A **80**, 012314 (2009).
[16] G. Adesso and I. Fuentes-Schuller, Quant. Inf. Comput. **9**, 0657 (2009).
[17] P. C. W. Davies, J. Phys. A **8**, 609 (1975).
[18] W. G. Unruh, Phys. Rev. D **14**, 870 (1976).
[19] S. Takagi, Prog. Theor. Phys. Suppl. **88**, 1 (1986).
[20] L. C. B. Crispino, A. Higuchi, and G. E. A. Matsas, Rev. Mod. Phys. **80**, 787 (2008).
[21] E. Martín-Martínez and J. León, Phys. Rev. A **80**, 042318 (2009).
[22] C. W. Misner, K. S. Thorne, and J. A. Wheeler, *Gravitation* (Freeman, San Francisco, 1973).
[23] N. D. Birrell and P. C. W. Davies, *Quantum Fields in Curved Space* (Cambridge University, New York, 1984).
[24] R. Jáuregui, M. Torres, and S. Hacyan, Phys. Rev. D **43**, 3979 (1991).
[25] M. B. Plenio, Phys. Rev. Lett. **95**, 090503 (2005).
[26] J. Schliemann, J. I. Cirac, M. Kus, M. Lewenstein, and D. Loss, Phys. Rev. A **64**, 022303 (2001).
[27] G. C. Ghirardi and L. Marinatto, Phys. Rev. A **70**, 012109 (2004).